HHS Public Access

Author manuscript

Oncogene. Author manuscript; available in PMC 2022 December 30.

Published in final edited form as:

Oncogene. 2022 June ; 41(24): 3370–3380. doi:10.1038/s41388-022-02345-3.

Histone H3K9 Methyltransferase SETDB1 Augments Invadopodia Formation to Promote Tumor Metastasis

Shuhei Ueshima[1], **Jia Fang**[1,*]

[1]Department of Pharmacology & Therapeutics, Roswell Park Comprehensive Cancer Center, Elm & Carlton Streets, Buffalo, NY 14263

Abstract

Non-small cell lung cancer (NSCLC) is one of leading causes of cancer-related mortality worldwide, which harbors various accumulated genetic and epigenetic abnormalities. Histone methyltransferase SETDB1 is a pivotal epigenetic regulator whose focal amplification and upregulation are commonly detected in NSCLC. However, molecular mechanisms underlying the pro-oncogenic function of SETDB1 remain poorly characterized. Here, we demonstrate that SETDB1 augments the migration and invasion capabilities of NSCLC cells by reinforcing invadopodia formation and mediated ECM degradation. At the molecular level, SETDB1 suppresses the expression of FOXA2, a crucial tumor and metastasis suppressor via coordinated epigenetic mechanisms – SETDB1 not only catalyzes histone H3K9 methylation on FOXA2 genomic locus, but also recruits DNMT3A to regulate DNA methylation on CpG island. Consequently, depletion of Setdb1 in murine lung adenocarcinoma cells completely abolished their full and spontaneous metastatic capabilities in mouse xenograft models. These findings together establish the pro-metastasis activity of SETDB1 in NSCLC and elucidate the underlying cellular and molecular mechanisms.

Introduction

Non-small cell lung cancer (NSCLC) is one of the most common malignancies and the leading cause of cancer-related deaths worldwide. The high mortality of NSCLC patients is associated with tumor metastasis, relapse, resistance to therapy and the common diagnosis at advantaged stages [1]. As a heterogeneous disease, NSCLC development is a result of accumulated genetic and epigenetic abnormalities. Over the past decades, identification of oncogenic driver mutations in NSCLC led to targeted therapeutics which have achieved clear clinical benefits in several circumstances [2]. Meanwhile, epigenetic modifications, including histone modifications and DNA methylation have also emerged as crucial regulators during NSCLC development [3].

[*]Correspondence and requests for materials should be addressed: J.F. (Jia.Fang@RoswellPark.org), Phone: 716-845-2926, Fax: 716-845-8857.

Author Contributions

J.F. conceived the project, designed the experiments, and wrote the manuscript. S.U. carried out the experiments and analyzed data.

Competing Interests statement: The authors declare no potential competing interests.

SETDB1 (also known as KMT1E or ESET) is a key member of the SUV39 subfamily histone methyltransferases [4], which introduces H3K9 tri-methylation on euchromatin [5], transposable elements (TEs) [6] and telomeres [7]. SETDB1 contributes to various physiological processes, such as early development [8], endogenous retroviruses (ERV) silencing [6], intestinal epithelial differentiation [9] and immune cell function [10]. The focal amplification of SETDB1 was also detected in multiple cancers, suggesting it has a pro-oncogenic function [11, 12]. In NSCLC, database analyses revealed a significant global SETDB1 upregulation [13] and transcriptomic divergence between SETDB1-high and SETDB1-low tumors [14], indicating that SETDB1-mediated transcriptional dysregulation is important for NSCLC development. Consistently, SETDB1 overexpression in NSCLC cells promotes in vitro proliferation and xenograft tumor growth through different pathways, including WNT signaling activation, p53 repression, AKT1 methylation, etc [15]. Recent studies also demonstrated that SETDB1-mediated TE silencing enables tumor cells to evade immune surveillance [16, 17] and to tolerate lethal-dose drug treatment [18]. Prognostic analysis of a cohort of stage I NSCLC patients after complete surgical resection revealed a significant correlation between high SETDB1 expression and tumor relapse and poorer survival. Furthermore, 40% recurrences showed exclusive or concomitant distant metastases [19], suggesting that SETDB1 upregulation could facilitate NSCLC malignant progression. Intriguingly, database analysis revealed a significantly inverse correlation between elevated SETDB1 expression and epithelial-mesenchymal transition (EMT) in NSCLC [14] while discrepancies in SETDB1-mediated regulation of NSCLC cell invasion have also been well documented [12, 20]. Therefore, the contribution of SETDB1 in NSCLC malignant progression and metastasis is largely ambiguous while dissecting the mechanisms of action is critical to further clarify its functional significance.

During malignant progression, NSCLC cells acquire abilities to penetrate the basement membrane, intravasate into the circulation and extravasate to distal organs. It has emerged that invadopodia, the actin-rich membrane protrusions coordinate local adhesions and proteases to degrade extracellular matrix (ECM) and facilitate migration and invasion [21]. Consistently, upregulation of core invadopodia component TKS5 is correlated with poor survival of NSCLC patients diagnosed at early stages [22]. Using $Kras^{G12D/+};p53^{fl/fl}$ mouse lung adenocarcinoma model, another study demonstrated that Tks5 is repressed in non-metastatic tumor cells by pioneer transcription factor Foxa2 and lineage-specific factors Nkx2–1 and Cdx2. Synergetic loss of these factors fully activates metastatic program and associates with poor prognosis [23]. Although FOXA2 mutations were rare in human NSCLC, it is frequently silenced, likely via epigenetic mechanisms [24, 25]. However, mechanisms underlying FOXA2 epigenetic silencing during malignant progression of NSCLC remain enigmatic.

Here, we report that SETDB1 strengthens NSCLC cell migratory and invasive abilities by promoting invadopodia formation and ECM degradation. It is accomplished by epigenetic silencing of key metastasis suppressor FOXA2 through SETDB1-mediated H3K9 trimethylation, as well as DNMT3A recruitment and DNA methylation. In xenograft models, we demonstrate that Setdb1 is essential to maintain the full and spontaneous metastatic capabilities of murine $Kras^{G12D/+};p53^{fl/fl}$ lung adenocarcinoma cells to form

the lung metastases from the subcutaneous tumors. These findings together establish the pro-metastasis activity of SETDB1 in NSCLC and elucidate the underlying mechanisms.

Materials and Methods

Cell lines, Antibodies, and Inhibitors

293T cells (ATCC) and murine *Kras*$^{G12D/+}$;*p53*$^{fl/fl}$ lung adenocarcinoma Tnonmet, Tmet and Met cells [26] were cultured in DMEM with 10% FBS and penicillin/streptomycin (Corning). H1299, H2009, H23 and H157 cell lines (ATCC) were cultured in RPMI-1640 with FBS and penicillin/streptomycin. SETDB1 antibodies were derived from rabbit using purified antigens [21–185aa (N) or 900–1152aa (C)] and affinity purified from serum. MPP8 antibody was described [27] while antibodies against GAPDH (Proteintech), E-cadherin (BD), N-cadherin (BD), Cortactin (Millipore), FOXA2 (Cell Signaling & Abcam), Histone H3 (Abcam), Histone H3K9me3 (Abcam), Flag (Sigma), DNMT3A (Cell Signaling), normal IgG and secondary antibodies (Jackson Immuno) were from commercial sources. Decitabine and GSK126 were from Sigma and Cayman Chemical.

Mouse and Xenografts

All animal care and experiments were approved by the Institutional Animal Care and Use Committee (IACUC). For xenografts, ~1.25×10^4 $Tmet_{373T1}$ cells stably expressing luciferase were resuspended in DMEM and subcutaneously injected into the left hind flank of randomized male SCID mice (*C.B-Igh-1bIcrTac-Prkdcscid/Ros*, 8wks). Primary tumors were developed up to ~2cm in diameter while tumor size was measured by a caliper periodically. For in vivo bioluminescence imaging (IVIS Spectrum imager), mice were i.p. injected with 10 μL/g body weight D-luciferin (Goldbio, 15 mg/ml in PBS). At the endpoint, lungs were also harvested for ex vivo imaging. Bioluminescence was quantified (Living Image software, PerkinElmer) as total flux (photos/sec) and average radiance (total flux/cm^2/Sr) were calculated. Primary tumors and lungs were also embedded, sectioned and stained with Hematoxylin and Eosin. For immunohistochemistry (IHC), paraffin sections were treated with 3% H_2O_2 and blocked by 10% goat serum after antigen retrieval with sodium citrate. After incubating with SETDB1 or FOXA2 antibody and biotinylated 2nd antibodies sequentially, sections were developed with diaminobenzidine (DAB) and mounted.

Invadopodia and ECM Degradation Assays

For invadopodia, cells were fixed (4% paraformaldehyde), permeabilized (0.1% Triton X-100), blocked (1% BSA) and then stained with Cortactin antibody and DyLight-488-conjugated 2nd antibody. Cells were next incubated with Alexa-594-conjugated phalloidin (Invitrogen) followed by DAPI (Sigma) before microscopy. For ECM degradation, poly-L-lysine (MP Biomed) treated coverslips were coated with solution containing 1:9 ratio of 0.1% FITC-gelatin (Invitrogen) and 0.2% plain gelatin (Sigma) followed by crosslinking with 0.8% glutaraldehyde. After extensive wash, cells ($0.6–1\times10^5$) were seeded and treated with 5 μM Batimastat (Sigma, 16 hr plus 4–8 hr after removal) or DMSO (8 hr) before immunofluorescence procedures. Images were taken at 10 random fields per sample (~100–400 cells) while degradation area was quantified by ImageJ as described [28].

RNA sequencing

cDNA libraries were synthesized using 1μg RNA purified from biological triplicates of control or SETDB1-KO H1299 cells using commercial kits (Illumina, Qiagen) and then sequenced via 75 nucleotide paired-end running on Illumina HiSeq 2000. The reads were aligned to the human genome (GRCh38.p7) and GENCODE (v25). Mapped reads were quantified at the gene level using HTSeq and non-empty overlap option. DEseq2 was used to call differentially expressed genes (DEGs) while GSEA (v3.0) was used for pathway analysis of DEGs.

DNA Methylation Analysis

MethylScreen was carried out as described [29]. Briefly genomic DNA were digested by McrBC (MDRE), a mixture of HhaI, HpyCH4IV and AciI (MSRE) or both MDRE and MSRE (double digestion) for 16 h at 37°C followed by enzyme inactivation. qPCR was then performed in triplicates while the results were calculated accordingly to determine different CpG methylation states.

Statistical Analysis

For migration, invasion and ChIP assays, the *p*-value was determined using two-tailed Student's *t*-test. For ECM degradation assays, statistical analyses were performed using one-way ANOVA and Tukey's test as described [28]. For mouse xenografts, non-parametric two-tailed Mann-Whitney test was utilized. All analyses were performed using Microsoft Excel.

Other Assays

Details for other assays including CRISPR/Cas9 knockout, knockdown, immunoprecipitation, cell proliferation, wound-healing, migration, and invasion assays, etc., sequence information for sgRNAs, shRNAs, qPCR, and ChIP are available in the Supplementary information Online.

Results

SETDB1 promotes migration and invasion of NSCLC cells

To better understand the functional importance of SETDB1 upregulation in NSCLC, we knocked-out SETDB1 using CRISPR/Cas9 in a panel of NSCLC cells with various backgrounds, including H1299 (carcinoma), H23 (adenocarcinoma, LUAD), H2009 (adenocarcinoma, LUAD), H157 (squamous-cell carcinoma, LUSC) (Fig.1A). While different SETDB1-KO cells displayed a negligible to moderate proliferation reduction (Fig.1B), they all exhibited a significantly slower recovery in the scratch wound-healing assays (Fig.1C), suggesting that SETDB1 plays a critical and more consistent role in regulating motility of NSCLC cells than proliferation. To further test this possibility, we performed the Boyden chamber assays and quantitated their abilities to move through transwell membranes with or without Matrigel coating. Comparing with controls, all SETDB1-KO cells exhibited a significant reduction on the migratory (43~76%) and invasive (53~92%) capabilities (Fig.1D, Supplemental Fig.1). Thus, SETDB1 plays a more universal

role in regulating NSCLC cell migration and invasion and could thus contribute to tumor progression.

SETDB1 promotes invadopodia formation and ECM degradation

Increased migration and invasion is a key characteristic of EMT which is often associated with metastatic potential of epithelial cancer cells [30]. To test whether SETDB1 depletion induced an EMT reversal, we examined cell surface markers. Unexpectedly, SETDB1 knockout failed to reactivate epithelial marker E-cadherin and only downregulated mesenchymal marker N-cadherin in H1299 cells (Fig.2A), suggesting that reduced motility and invasiveness of SETDB1-KO cells are caused by different mechanisms. To dissect molecular details, we profiled transcriptome changes in control and SETDB1-KO H1299 cells by RNA-Sequencing (RNA-Seq). Differential expression and gene set enrichment analyses (GSEA) uncovered that multiple top downregulated processes in SETDB1-KO cells are cancer- and ECM- related pathways (Fig.2B, Supplemental Fig.2A-C). Intriguingly, many top downregulated genes are associated with matrisome pathways (supplemental Fig.2B-D). Among them we confirmed that TNC, ADAM12, ADAM19 and $TKS5_{long}$ are substantially downregulated upon SETDB1 depletion by RT-PCR (Fig.2C). As these proteins have been implicated in metastasis and poor prognosis of different cancers [31, 32], these findings indicate that SETDB1 could regulate migration and invasion of NSCLC cells through modulating ECM function.

As the members of a disintegrin and metalloproteinases (ADAM) family, ADAM12 and ADAM19 have been shown to interact with invadopodia scaffolding protein TKS5 and localize to podosomes in Src-transformed cells [33]. Recent studies also reported the key role of ADAM12 and TNC in invadopodia formation, ECM degradation and metastasis of breast cancer [34] and Ewing sarcoma [35]. We thus assessed whether SETDB1 could modulate invadopodia function. Invadopodia are transient adhesive membrane protrusions which coordinate ECM degradation and tumor cell invasion [36] and are commonly identified by the colocalization of F-Actin with Actin-bundling protein Cortactin [37]. In our immunofluorescence analysis, ~68% of control-KO cells displayed F-Actin and Cortactin colocalized invadopodia whereas only ~34% SETDB1-KO cells exhibited similar structures (Fig.2D-E). To validate these results, we analyzed H157 cells which also form detectable invadopodia [28]. Similarly, invadopodia occurrence reduced robustly from ~28% to ~5% upon SETDB1 knockout (Fig.2F-G), demonstrating that SETDB1 promotes invadopodia formation in NSCLC cells. To determine whether SETDB1-sustained invadopodia occurrence has functional outcomes, we performed the FITC-gelatin degradation assay [38]. Consistently, SETDB1 depletion led to a forceful reduction (~70%) on FITC-gelatin degradation mediated by H1299 cells (Fig.2H-I). Moreover, H157 cells mediated ECM (FITC-gelatin) degradation was largely abolished (>98% reduction) upon SETDB1 knockout (Fig2J-K). Together, these findings establish the functional role of SETDB1 in promoting invadopodia formation in NSCLC cells and further demonstrate that SETDB1-sustained invadopodia actively degrade ECM and could in turn promote migration and invasion.

SETDB1 represses tumor and metastasis suppressor FOXA2

Although invadopodia-related genes ADAM12, ADAM19 and TNC are downregulated in SETDB1-KO cells, they are not likely the direct targets of SETDB1 due to the repressive nature of H3K9 methylation. We then examined multiple upregulated genes from our RNA-Seq data and confirmed the upregulation of several tumor-suppressing transcriptional factors by RT-PCR in SETDB1-KO cells (Fig.3A). Among them, pioneer transcription factor FOXA2 (up >250 fold) is one of the most upregulated gene (Supplemental Fig.2D) and has been shown to repress $Tks5_{long}$ expression and impede metastases of murine lung adenocarcinoma [23]. Similarly, a robust increase of FOXA2 protein was also detected in other SETDB1-KO NSCLC cells (Fig.3B), which is accompanied by a forceful downregulation of invadopodia-related genes we identified (Supplemental Fig.3A-B), indicating that the simultaneous FOXA2 repression and invadopodia gene upregulation induced by SETDB1 could be a general mechanism in NSCLC cells. To test whether SETDB1 directly suppresses FOXA2 expression, we examined SETDB1 localization on FOXA2 genomic locus by ChIP assays. As shown in Fig.3C, a distinct SETDB1 enrichment was readily detected on FOXA2 proximal promoter in control cells but was greatly impaired in SETDB1-KO cells. Intriguingly, SETDB1 exhibited similar enrichment in −2kb upstream and +2kb downstream regions in control but not SETDB1-KO cells, suggesting that it could occupy a broader chromatin domain. We further applied a different SETDB1 antibody to ChIP assays and obtained similar results which validated the specificity of SETDB1 targeting on FOXA2 gene locus. Moreover, SETDB1 occupancy in these regions is accompanied by a robust enrichment of H3K9me3 which is abolished upon SETDB1 depletion. Meanwhile, nucleosome structure measured by histone H3 occupancy only changed slightly (Fig.3D). Together, these findings demonstrate that SETDB1 directly targets FOXA2 gene locus and catalyzes H3K9me3 in a broader chromatin domain to suppress gene expression.

To assess the importance of SETDB1-mediated FOXA2 silencing in phenotypic changes observed in NSCLC cells, we first overexpressed FOXA2 in H1299 cells and detected a forceful downregulation of ADAM12/19 and TNC (Fig.3E), indicating these invadopodia-related genes could be downstream factors of FOXA2. To investigate this regulation at the endogenous level, we next stably expressed shRNA against a scramble sequence (control) or FOXA2 in SETDB1-KO H1299 cells. While FOXA2 reactivation induced by SETDB1-KO was abrogated by FOXA2 knockdown (FOXA2-KD), a notable upregulation of these invadopodia-related genes is readily detected (Fig.3F-G). Importantly, the scratch wound-healing ability of SETDB1-KO H1299 was also greatly restored (Fig.3H). We further determined the impact of additional FOXA2-KD on migration and invasion using the transwell assays and uncovered that FOXA2 loss significantly retrieved cell migration and invasion capabilities inhibited by SETDB1-KO (Fig.3I). Together, we conclude that SETDB1-sustained NSCLC cell migration and invasion are largely mediated through epigenetic silencing of FOXA2.

SETDB1 cooperates with DNA methylation for FOXA2 epigenetic silencing

FOXA2 expression is inversely correlated with DNA hypermethylation in NSCLC cells [24, 25], whereas a subset of Setdb1 also colocalizes with Polycomb Repressive Complex 2

(PRC2) to repress developmental genes [39]. We then asked whether SETDB1 cooperates with DNA methylation and/or PRC2 for FOXA2 gene silencing. To test this possibility, we treated control and SETDB1-KO H1299 cells with a DNA demethylating agent decitabine (DEC) or a potent EZH2 inhibitor GSK126. In control cells, we detected a notable dosage-dependent increase of FOXA2 protein upon decitabine treatment but not GSK126. In SETDB1-KO cells, decitabine-induced FOXA2 upregulation was inconclusive, likely due to substantial FOXA2 reactivation (Fig.4A). Furthermore, RT-PCR analysis reported a significant 8.8-fold and 18.6-fold increase of FOXA2 mRNA with 2μM and 10μM decitabine treatment respectively but only a modest 2.5-fold increase with 10μM GSK126, indicating that DNA methylation plays a more critical role in mediating FOXA2 silencing than PRC2-catalyzed H3K27me3 (Fig.4B). Furthermore, decitabine treatment only induced 1.2~2.7-fold increase of FOXA2 mRNA in SETDB1-KO cells (Fig.4B). Therefore, these results suggest that SETDB1 and DNA methylation are major repressive epigenetic mechanisms for FOXA2 silencing and could contribute to the same repression pathway.

Due to previously reported crosstalk between SETDB1 and DNA methylation [40, 41], we further analyzed DNA methylation in FOXA2 CpG island using MethylScreen approach [29] to determine whether SETDB1 modulates DNA methylation on FOXA2 locus. We focused on three CpG clusters in the 5'-region of the longest FOXA2 CpG island [42] as their hypermethylation was correlated with FOXA2 repression [24]. In control cells, all three CpG clusters are methylated, ranging from 44.6% to 94.6%. Upon SETDB1 loss, however, DNA methylation reduced slightly in CpG cluster 1 (9.7%) but decreased forcefully in cluster 2 (23.9%) and 3 (52.7%) while DNA hypomethylation increased accordingly (Fig.4C), suggesting SETDB1 indeed modulates DNA methylation in these regions. To dissect underlying mechanisms, we assessed protein interactions between SETDB1 and three DNMTs by immunoprecipitation (IP)-coupled western blot analysis. Only DNMT3A exhibited robust and specific interactions with endogenous SETDB1 and MPP8 (control [27]) (Fig.4D). To determine whether SETDB1 recruits DNMT3A onto FOXA2 CpG clusters for DNA methylation, we examined their occupancy in these CpG clusters by ChIP assays. As shown in Fig.4E-G, a significant enrichment of SETDB1 and H3K9me3 was readily detected in CpG cluster 2 and 3 but not cluster 1, and these enrichments were abolished by SETDB1 knockout. Strikingly, similar DNMT3A occupancy was observed in CpG cluster 2 and 3 in control cells but disappeared in SETDB1-KO cells. Given the localization changes of SETDB1, H3K9me3 and DNMT3A are greatly correlated with DNA methylation alterations in SETDB1-KO cells, we conclude that SETDB1 recruits DNMT3A, likely through their protein interactions to modulate DNA methylation for epigenetic silencing of FOXA2.

Setdb1 represses Foxa2 and promotes migration and invasion of murine lung adenocarcinoma cells

Foxa2, together with Nkx2–1 and Cdx2 serve as key regulatory nodes to inhibit malignant progression of mouse $Kras^{G12D/+};p53^{fl/fl}$ lung adenocarcinoma and are responsible for one-third of transcriptome changes [23]. We thus examined Setdb1 and Foxa2 expressions in a serial of cell lines derived from this model [22, 26]. Consistent with prior report [23], Foxa2 is highly expressed in Tnonmet cells (non-metastatic primary tumors) but drastically

downregulated in Tmet (metastatic primary tumors) and Met (metastases) cells. In contrast, Setdb1 is weakly expressed in all Tnonmet cell lines but robustly upregulated in Tmet and Met cells (Fig.5A). To test whether Foxa2 downregulation in metastatic Tmet cells is caused by Setdb1 upregulation, we knocked-out Setdb1 in $Tmet_{373T1}$ cells using CRISP/Cas9 and detected a substantial increase of Foxa2 protein (Fig.5B) which is accompanied by a modest reduction of cell proliferation (Fig.5C). To further evaluate our working model, we investigated whether Setdb1 loss modulates the metastatic potential of these murine lung adenocarcinoma cells. While the motility of $Tmet_{373T1}$ cells decreased significantly upon Setdb1 knockout in the scratch wound-healing assay, their migratory and invasive abilities reduced substantially at ~54% and ~82% respectively in the transwell assays (Fig.5D-E). In addition, Setdb1 loss resulted in a forceful downregulation of invadopodia-related genes ADAM12/19 and $Tks5_{long}$ (Fig.5F). Therefore, depletion of Setdb1 also de-represses Foxa2 expression in mouse $Tmet_{373T1}$ cells and abrogates the metastatic potential of these cells. Given that these results phenocopied changes detected in human SETDB1-KO NSCLC cells (Fig.1), SETDB1-mediated FOXA2 repression and the subsequent regulation on migration and invasion could represent a general mechanism for modulating metastatic potential of NSCLC cells.

Setdb1 is essential for malignant progression and metastasis of murine lung adenocarcinoma

Metastatic Tmet cell lines derived from $Kras^{G12D/+};p53^{fl/fl}$ murine lung adenocarcinomas possess the ability to disseminate from the primary tumor site and form lung metastasis nodules after being subcutaneously transplanted into immune-compromised mice [22, 23]. We further utilized this model and investigated the functional importance of Setdb1 in lung adenocarcinoma progression and metastasis in vivo using xenograft models. To monitor tumor development and metastasis noninvasively, we stably expressed luciferase in control and two Setdb1-KO $Tmet_{373T1}$ cell lines (Supplemental Fig.5A) and subcutaneously transplanted them (~1.25×10^4 cells) into SCID mice. Control tumors developed rapidly and reached the endpoint at day 32, where two Setdb1-KO tumors were about half of the volume and reached the endpoint at day 40 (Fig.6A), suggesting that Setdb1 loss modestly reduced tumor growth in vivo. Immunohistochemistry and western blot analyses of endstage primary tumors further confirmed the inverse correlation between Foxa2 and Setdb1 expression (Fig.6B-C). Intriguingly, Setdb1-KO tumor cells apparently adapted a more cuboidal epithelial morphology while control tumor cells predominantly showed a mesenchymal morphology (Fig.6B), indicating the invasiveness of $Tmet_{373T1}$ cells was mitigated in vivo upon Setdb1 depletion. However, a reversed EMT marker expression was not detected by western blot (Fig.6C). More importantly, control tumors rapidly disseminated from the subcutaneous sites and aggressively metastasized into the lungs. In sharp contrast, no detectable lung metastasis was developed from Setdb1-KO tumors even after they reached the similar size at the endpoint (Fig.6D-E, Supplemental Fig.5B). To further validate the results, we dissected the lungs from the endstage mice and following ex vivo bioluminescence imaging quantification and H&E histology analyses revealed that Setdb1 depletion completely abolished the spontaneous metastatic ability of $Tmet_{373T1}$ cells in these xenograft models (Fig.6F-G, Supplemental Fig.5C). Moreover, a substantial downregulation of invadopodia-related genes Adam12/19 and Tnc was

readily detected in Setdb1-KO primary tumors (Fig.6H). Using similar xenograft models, previous study has shown that knockdown of Foxa2 in mouse non-metastatic lung cancer (Tnonmet) cells significantly increased lung metastasis nodules, whereas knockdown of Foxa2, Cdx2 and Nkx2–1 altogether further promoted this effect [23]. Therefore, our xenograft results together with in vitro findings (Fig.3F-I, Fig.5D-F) suggest that loss of spontaneous metastasis capability of Setdb1-KO $Tmet_{373T1}$ cells is, at least in part due to de-repressed Foxa2 expression. Together, our in vivo findings further demonstrate the functional importance of Setdb1-Foxa2 regulatory node in NSCLC malignant progression and metastasis.

Discussion

Although SETDB1 upregulation was frequently observed in NSCLC and multiple other human cancers, prior studies largely focused on its role in regulating tumor cell proliferation in vitro and in vivo through various molecular pathways. In this study, we present evidence in vitro and in vivo that together depict the pro-metastatic activity of SETDB1 in NSCLC. Specifically, SETDB1 augments migratory and invasive capabilities of tumor cells via promoting invadopodia formation and ECM degradation. As the result, Setdb1 is a prerequisite to sustain the full and spontaneous metastatic capabilities of tumor cells derived from murine $Kras^{G12D};p53^{fl/fl}$ lung adenocarcinomas in xenograft models. We also present molecular evidence which demonstrate that SETDB1-sustained NSCLC cell migration and invasiveness are mediated through epigenetic silencing of key metastasis suppressor FOXA2. In addition to catalyzing H3K9 trimethylation on FOXA2 genomic locus, SETDB1 recruits DNMT3A for DNA methylation to reinforce gene silencing. Together, we established the functional significance of SETDB1 in NSCLC malignant progression and metastasis and elucidated the underlying mechanisms.

The airway transcription factor FOXA2 is ubiquitously expressed in normal bronchial epithelial cells and type II pneumocytes and plays a crucial role in alveolarization and airway epithelial cell differentiation [43]. In contrast, loss or reduced FOXA2 expression was commonly detected in human primary NSCLC tissues, including both adenocarcinomas and squamous cell carcinomas [24]. IHC analyses of 130 annotated stage I lung adenocarcinomas also confirmed the frequent FOXA2 downregulation (52.9%) and revealed a trend favoring survival in patients with high FOXA2 expression [24]. These results suggest that FOXA2 functions as a bona fide tumor suppressor. In murine lung adenocarcinomas, a stringent inverse-correlation of Foxa2 level to tumor grade was observed, which further highlights the key role of Foxa2 as a safeguard against malignant progression of NSCLC [23]. Intriguingly, another gene expression analysis of 64 stage I human primary NSCLC samples reported SETDB1 as a strong independent prognostic factor of tumor recurrence while high SETDB1 expression is significantly associated with shorter disease-free survival [19]. Although the direct correlation between frequent FOXA2 loss and SETDB1 upregulation in human NSCLC and other cancers is unknown and warrants further investigation, our findings are in line with these prior studies which clearly illustrate that SETDB1 and FOXA2 have opposite functions in NSCLC.

FOXA2 has been shown to inhibit EMT of NSCLC and breast cancer cells by repressing SLUG and ZEB2 respectively [44, 45]. However, it promotes EMT of colon cancer cells and is upregulated in advanced tumor stage [46], suggesting EMT regulation by FOXA2 could be largely context dependent. In different NSCLC cells and xenograft tumors, SETDB1-KO induced FOXA2 reactivation failed to upregulate E-cadherin expression (Fig.2A, 6C). In contrast, direct or indirect modulation of FOXA2 level resulted in inverse changes on expression of several invadopodia-related genes in vitro and in vivo (Fig.3E, 3G, 5F, 6H).Considering the role of invadopodia in metastatic invasion and the established function of Foxa2 in impeding malignant progression of mouse lung adenocarcinoma [22, 23], our findings together support a model in which SETDB1 represses FOXA2 expression to upregulate these invadopodia-related genes and promote NSCLC cell migration and invasion via ECM degradation, and thus augments metastatic progression. In this case, morphologic changes of Setdb1-KO primary tumor cells could be the results of reduced actin bundling in invadopodia instead of EMT reversal. The relevance of identified SETDB1-FOXA2 regulatory node in human NSCLC tissues and mechanisms underlying the regulation of these invadopodia-related genes by FOXA2 is currently under investigation. Intriguingly, a recent screening identified SIRT6 as an ADAM12 co-repressor [47] while SIRT6 interacts with FOXA2 to suppress ZEB2 expression in hepatocellular carcinoma cells [48]. These results suggest that FOXA2 could repress EMT-inducing transcription factors and/or invadopodia related genes in different tumor types through similar or different mechanisms to mitigate their migration and invasion abilities.

The crosstalk of SETDB1-DNMT3A on FOXA2 silencing in NSCLC cells elucidates a coordinated action by multiple chromatin modifiers. It is consistent with recent transcriptomic analyses showing that SETDB1-high NSCLC has overrepresented DNMT expression, especially DNMT3A [14]. Intriguingly, decitabine-induced FOXA2 de-repression is substantially lower than SETDB1 depletion did (Fig.3A, 4A-B). We thus propose that SETDB1 plays the primary role to suppress FOXA2 gene expression via histone H3K9 methylation while it also recruits DNMT3A for DNA methylation to reinforce epigenetic silencing. However, SETDB1-DNMT3A interplay could be more complex than the simple recruitment model. For instance, we and others revealed that SETDB1 interacts with H3K9me3-binding proteins MPP8 [27] and HP1 [49, 50] while these interactions have been shown to recruit DNMTs to target promoters and modulate DNA methylation. Thus, DNMT3A enrichment on FOXA2 CpG island could also rely on SETDB1-catalyzed H3K9me3 and subsequent binding by MPP8 and/or HP1, which could further sustain SETDB1 occupancy to facilitate the spreading of H3K9me3 and DNA methylation into large chromatin domains. As SETDB1 forms a stable complex with MBD1 and ATF7IP [51], DNMT3A-mediated CpG methylation may be recognized by MBD1 which may also contribute to retention of SETDB1-centered epigenetic complex on FOXA2 genomic locus as a feedforward regulation. Together, multiple epigenetic events could result in formation of a broader domain of facultative heterochromatin to maintain long-term transcription silencing in NSCLC cells. Although Setdb1 also coordinates with PRC2 and H3K27me3 to repress multiple developmental genes in mESCs [39], this interplay was not evident on FOXA2 silencing in NSCLC cells, suggesting that SETDB1-centered epigenetic repression pathways in NSCLC progression could be different from physiological processes and

context dependent. As expression of multiple epigenetic players is overrepresented in SETDB1-high NSCLCs [14], SETDB1 may coordinate a large epigenetic network for transcription reprogramming to facilitate NSCLC progression and metastasis.

Supplementary Material

Refer to Web version on PubMed Central for supplementary material.

Acknowledgments

We thank Dr. Tyler Jacks for murine lung adenocarcinoma cell lines, Dr. Shengyu Yang for technical assistance with invadopodia assays, Dr. David Goodrich for constructive discussion and suggestions and support from Roswell Park Comprehensive Cancer Center (RPCCC) Shared Resources, including BIOINFO, GSR, TISR and LASR. This project was supported, in part, by grants from the NIH (CA172774) and Roswell Park Alliance Foundation (all to J.F.), and by RPCCC and NCI center grant P30CA016056.

Data availability

The datasets generated and analyzed during the current study are available from the corresponding author on reasonable request.

References

1. Siegel RL, Miller KD, Jemal A. Cancer Statistics, 2017. CA Cancer J Clin 2017; 67: 7–30. [PubMed: 28055103]
2. Lee T, Lee B, Choi YL, Han J, Ahn MJ, Um SW. Non-small Cell Lung Cancer with Concomitant EGFR, KRAS, and ALK Mutation: Clinicopathologic Features of 12 Cases. J Pathol Transl Med 2016; 50: 197–203. [PubMed: 27086595]
3. Duruisseaux M, Esteller M. Lung cancer epigenetics: From knowledge to applications. Semin Cancer Biol 2018; 51: 116–128. [PubMed: 28919484]
4. Mozzetta C, Boyarchuk E, Pontis J, Ait-Si-Ali S. Sound of silence: the properties and functions of repressive Lys methyltransferases. Nat Rev Mol Cell Biol 2015; 16: 499–513. [PubMed: 26204160]
5. Dodge JE, Kang YK, Beppu H, Lei H, Li E. Histone H3-K9 methyltransferase ESET is essential for early development. Mol Cell Biol 2004; 24: 2478–2486. [PubMed: 14993285]
6. Fukuda K, Shinkai Y. SETDB1-Mediated Silencing of Retroelements. Viruses 2020; 12.
7. Gauchier M, Kan S, Barral A, Sauzet S, Agirre E, Bonnell E et al. SETDB1-dependent heterochromatin stimulates alternative lengthening of telomeres. Sci Adv 2019; 5: eaav3673.
8. Yuan P, Han J, Guo G, Orlov YL, Huss M, Loh YH et al. Eset partners with Oct4 to restrict extraembryonic trophoblast lineage potential in embryonic stem cells. Genes Dev 2009; 23: 2507–2520. [PubMed: 19884257]
9. Juznic L, Peuker K, Strigli A, Brosch M, Herrmann A, Hasler R et al. SETDB1 is required for intestinal epithelial differentiation and the prevention of intestinal inflammation. Gut 2021; 70: 485–498. [PubMed: 32503845]
10. Takikita S, Muro R, Takai T, Otsubo T, Kawamura YI, Dohi T et al. A Histone Methyltransferase ESET Is Critical for T Cell Development. J Immunol 2016; 197: 2269–2279. [PubMed: 27511731]
11. Ceol CJ, Houvras Y, Jane-Valbuena J, Bilodeau S, Orlando DA, Battisti V et al. The histone methyltransferase SETDB1 is recurrently amplified in melanoma and accelerates its onset. Nature 2011; 471: 513–517. [PubMed: 21430779]
12. Rodriguez-Paredes M, Martinez de Paz A, Simo-Riudalbas L, Sayols S, Moutinho C, Moran S et al. Gene amplification of the histone methyltransferase SETDB1 contributes to human lung tumorigenesis. Oncogene 2014; 33: 2807–2813. [PubMed: 23770855]

13. Cruz-Tapias P, Zakharova V, Perez-Fernandez OM, Mantilla W, Ram I-CS, Ait-Si-Ali S. Expression of the Major and Pro-Oncogenic H3K9 Lysine Methyltransferase SETDB1 in Non-Small Cell Lung Cancer. Cancers (Basel) 2019; 11.

14. Kang YK, Min B. SETDB1 Overexpression Sets an Intertumoral Transcriptomic Divergence in Non-small Cell Lung Carcinoma. Front Genet 2020; 11: 573515.

15. Strepkos D, Markouli M, Klonou A, Papavassiliou AG, Piperi C. Histone Methyltransferase SETDB1: A Common Denominator of Tumorigenesis with Therapeutic Potential. Cancer Res 2021; 81: 525–534. [PubMed: 33115801]

16. Zhang SM, Cai WL, Liu X, Thakral D, Luo J, Chan LH et al. KDM5B promotes immune evasion by recruiting SETDB1 to silence retroelements. Nature 2021; 598: 682–687. [PubMed: 34671158]

17. Griffin GK, Wu J, Iracheta-Vellve A, Patti JC, Hsu J, Davis T et al. Epigenetic silencing by SETDB1 suppresses tumour intrinsic immunogenicity. Nature 2021; 595: 309–314. [PubMed: 33953401]

18. Guler GD, Tindell CA, Pitti R, Wilson C, Nichols K, KaiWai Cheung T et al. Repression of Stress-Induced LINE-1 Expression Protects Cancer Cell Subpopulations from Lethal Drug Exposure. Cancer Cell 2017; 32: 221–237 e213. [PubMed: 28781121]

19. Lafuente-Sanchis A, Zuniga A, Galbis JM, Cremades A, Estors M, Martinez-Hernandez NJ et al. Prognostic value of ERCC1, RRM1, BRCA1 and SETDB1 in early stage of non-small cell lung cancer. Clin Transl Oncol 2016; 18: 798–804. [PubMed: 26542178]

20. Wu PC, Lu JW, Yang JY, Lin IH, Ou DL, Lin YH et al. H3K9 histone methyltransferase, KMT1E/SETDB1, cooperates with the SMAD2/3 pathway to suppress lung cancer metastasis. Cancer Res 2014; 74: 7333–7343. [PubMed: 25477335]

21. Saini P, Courtneidge SA. Tks adaptor proteins at a glance. J Cell Sci 2018; 131.

22. Li CM, Chen G, Dayton TL, Kim-Kiselak C, Hoersch S, Whittaker CA et al. Differential Tks5 isoform expression contributes to metastatic invasion of lung adenocarcinoma. Genes Dev 2013; 27: 1557–1567. [PubMed: 23873940]

23. Li CM, Gocheva V, Oudin MJ, Bhutkar A, Wang SY, Date SR et al. Foxa2 and Cdx2 cooperate with Nkx2–1 to inhibit lung adenocarcinoma metastasis. Genes Dev 2015; 29: 1850–1862. [PubMed: 26341558]

24. Basseres DS, D'Alo F, Yeap BY, Lowenberg EC, Gonzalez DA, Yasuda H et al. Frequent downregulation of the transcription factor Foxa2 in lung cancer through epigenetic silencing. Lung Cancer 2012; 77: 31–37. [PubMed: 22341411]

25. Halmos B, Basseres DS, Monti S, D'Alo F, Dayaram T, Ferenczi K et al. A transcriptional profiling study of CCAAT/enhancer binding protein targets identifies hepatocyte nuclear factor 3 beta as a novel tumor suppressor in lung cancer. Cancer Res 2004; 64: 4137–4147. [PubMed: 15205324]

26. Winslow MM, Dayton TL, Verhaak RG, Kim-Kiselak C, Snyder EL, Feldser DM et al. Suppression of lung adenocarcinoma progression by Nkx2–1. Nature 2011; 473: 101–104. [PubMed: 21471965]

27. Kokura K, Sun L, Bedford MT, Fang J. Methyl-H3K9-binding protein MPP8 mediates E-cadherin gene silencing and promotes tumour cell motility and invasion. EMBO J 2010; 29: 3673–3687. [PubMed: 20871592]

28. Pelaez R, Morales X, Salvo E, Garasa S, Ortiz de Solorzano C, Martinez A et al. beta3 integrin expression is required for invadopodia-mediated ECM degradation in lung carcinoma cells. PLoS One 2017; 12: e0181579.

29. Holemon H, Korshunova Y, Ordway JM, Bedell JA, Citek RW, Lakey N et al. MethylScreen: DNA methylation density monitoring using quantitative PCR. Biotechniques 2007; 43: 683–693. [PubMed: 18072598]

30. Sun L, Fang J. Epigenetic regulation of epithelial-mesenchymal transition. Cell Mol Life Sci 2016; 73: 4493–4515. [PubMed: 27392607]

31. Lowy CM, Oskarsson T. Tenascin C in metastasis: A view from the invasive front. Cell Adh Migr 2015; 9: 112–124. [PubMed: 25738825]

32. Nyren-Erickson EK, Jones JM, Srivastava DK, Mallik S. A disintegrin and metalloproteinase-12 (ADAM12): function, roles in disease progression, and clinical implications. Biochim Biophys Acta 2013; 1830: 4445–4455. [PubMed: 23680494]
33. Abram CL, Seals DF, Pass I, Salinsky D, Maurer L, Roth TM et al. The adaptor protein fish associates with members of the ADAMs family and localizes to podosomes of Src-transformed cells. J Biol Chem 2003; 278: 16844–16851. [PubMed: 12615925]
34. Eckert MA, Santiago-Medina M, Lwin TM, Kim J, Courtneidge SA, Yang J. ADAM12 induction by Twist1 promotes tumor invasion and metastasis via regulation of invadopodia and focal adhesions. J Cell Sci 2017; 130: 2036–2048. [PubMed: 28468988]
35. Hawkins AG, Julian CM, Konzen S, Treichel S, Lawlor ER, Bailey KM. Microenvironmental Factors Drive Tenascin C and Src Cooperation to Promote Invadopodia Formation in Ewing Sarcoma. Neoplasia 2019; 21: 1063–1072. [PubMed: 31521948]
36. Eddy RJ, Weidmann MD, Sharma VP, Condeelis JS. Tumor Cell Invadopodia: Invasive Protrusions that Orchestrate Metastasis. Trends Cell Biol 2017; 27: 595–607. [PubMed: 28412099]
37. Bowden ET, Onikoyi E, Slack R, Myoui A, Yoneda T, Yamada KM et al. Co-localization of cortactin and phosphotyrosine identifies active invadopodia in human breast cancer cells. Exp Cell Res 2006; 312: 1240–1253. [PubMed: 16442522]
38. Bowden ET, Coopman PJ, Mueller SC. Invadopodia: unique methods for measurement of extracellular matrix degradation in vitro. Methods Cell Biol 2001; 63: 613–627. [PubMed: 11060862]
39. Fei Q, Yang X, Jiang H, Wang Q, Yu Y, Yu Y et al. SETDB1 modulates PRC2 activity at developmental genes independently of H3K9 trimethylation in mouse ES cells. Genome Res 2015; 25: 1325–1335. [PubMed: 26160163]
40. Leung D, Du T, Wagner U, Xie W, Lee AY, Goyal P et al. Regulation of DNA methylation turnover at LTR retrotransposons and imprinted loci by the histone methyltransferase Setdb1. Proc Natl Acad Sci U S A 2014; 111: 6690–6695. [PubMed: 24757056]
41. Li H, Rauch T, Chen ZX, Szabo PE, Riggs AD, Pfeifer GP. The histone methyltransferase SETDB1 and the DNA methyltransferase DNMT3A interact directly and localize to promoters silenced in cancer cells. J Biol Chem 2006; 281: 19489–19500.
42. Bahar Halpern K, Vana T, Walker MD. Paradoxical role of DNA methylation in activation of FoxA2 gene expression during endoderm development. J Biol Chem 2014; 289: 23882–23892.
43. Wan H, Kaestner KH, Ang SL, Ikegami M, Finkelman FD, Stahlman MT et al. Foxa2 regulates alveolarization and goblet cell hyperplasia. Development 2004; 131: 953–964. [PubMed: 14757645]
44. Tang Y, Shu G, Yuan X, Jing N, Song J. FOXA2 functions as a suppressor of tumor metastasis by inhibition of epithelial-to-mesenchymal transition in human lung cancers. Cell Res 2011; 21: 316–326. [PubMed: 20820189]
45. Zhang Z, Yang C, Gao W, Chen T, Qian T, Hu J et al. FOXA2 attenuates the epithelial to mesenchymal transition by regulating the transcription of E-cadherin and ZEB2 in human breast cancer. Cancer Lett 2015; 361: 240–250. [PubMed: 25779673]
46. Wang B, Liu G, Ding L, Zhao J, Lu Y. FOXA2 promotes the proliferation, migration and invasion, and epithelial mesenchymal transition in colon cancer. Exp Ther Med 2018; 16: 133–140. [PubMed: 29896233]
47. Naciri I, Laisne M, Ferry L, Bourmaud M, Gupta N, Di Carlo S et al. Genetic screens reveal mechanisms for the transcriptional regulation of tissue-specific genes in normal cells and tumors. Nucleic Acids Res 2019; 47: 3407–3421. [PubMed: 30753595]
48. Liu J, Yu Z, Xiao Y, Meng Q, Wang Y, Chang W. Coordination of FOXA2 and SIRT6 suppresses the hepatocellular carcinoma progression through ZEB2 inhibition. Cancer Manag Res 2018; 10: 391–402. [PubMed: 29535552]
49. Fuks F. DNA methylation and histone modifications: teaming up to silence genes. Curr Opin Genet Dev 2005; 15: 490–495. [PubMed: 16098738]
50. Smallwood A, Esteve PO, Pradhan S, Carey M. Functional cooperation between HP1 and DNMT1 mediates gene silencing. Genes Dev 2007; 21: 1169–1178. [PubMed: 17470536]

51. Sarraf SA, Stancheva I. Methyl-CpG binding protein MBD1 couples histone H3 methylation at lysine 9 by SETDB1 to DNA replication and chromatin assembly. Mol Cell 2004; 15: 595–605. [PubMed: 15327775]

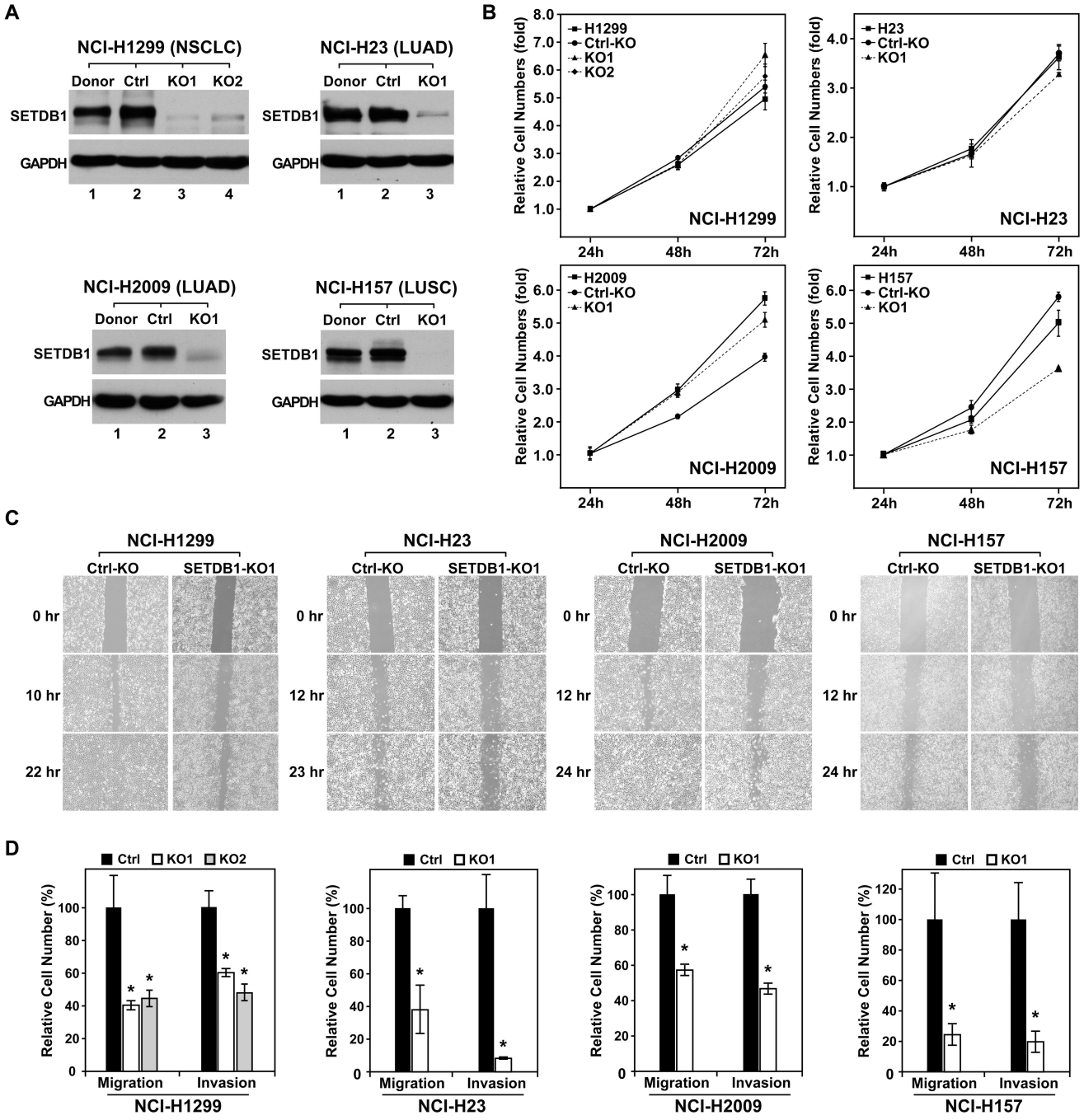

Figure 1.

SETDB1 promotes NSCLC cell migration and invasion. **(A)** Western blot analysis of control and SETDB1-KO H1299, H23, H2009 and H157 cells. **(B)** In vitro proliferation assays of indicated control and SETDB1-KO NSCLC cells using Cell Counting Kit-8. Cell number 24 h after seeding was normalized as 1. Results are from three independent samples (mean±s.d). **(C)** Wound-healing assays of various control and SETDB1-KO NSCLC cells. Cell monolayers were treated with 10 μg/ml Mitomycin C for 2 h before scratch while microscopy images were taken at indicated timepoints. **(D)** Transwell migration and

invasion assays of indicated control and SETDB1-KO NSCLC cells. Cells were treated with 10 μg/ml Mitomycin C for 2 h before being seeded into transwells. Results are from three independent samples (mean±s.d.). Control-KO cells were normalized as 100%. * indicates $p<0.05$.

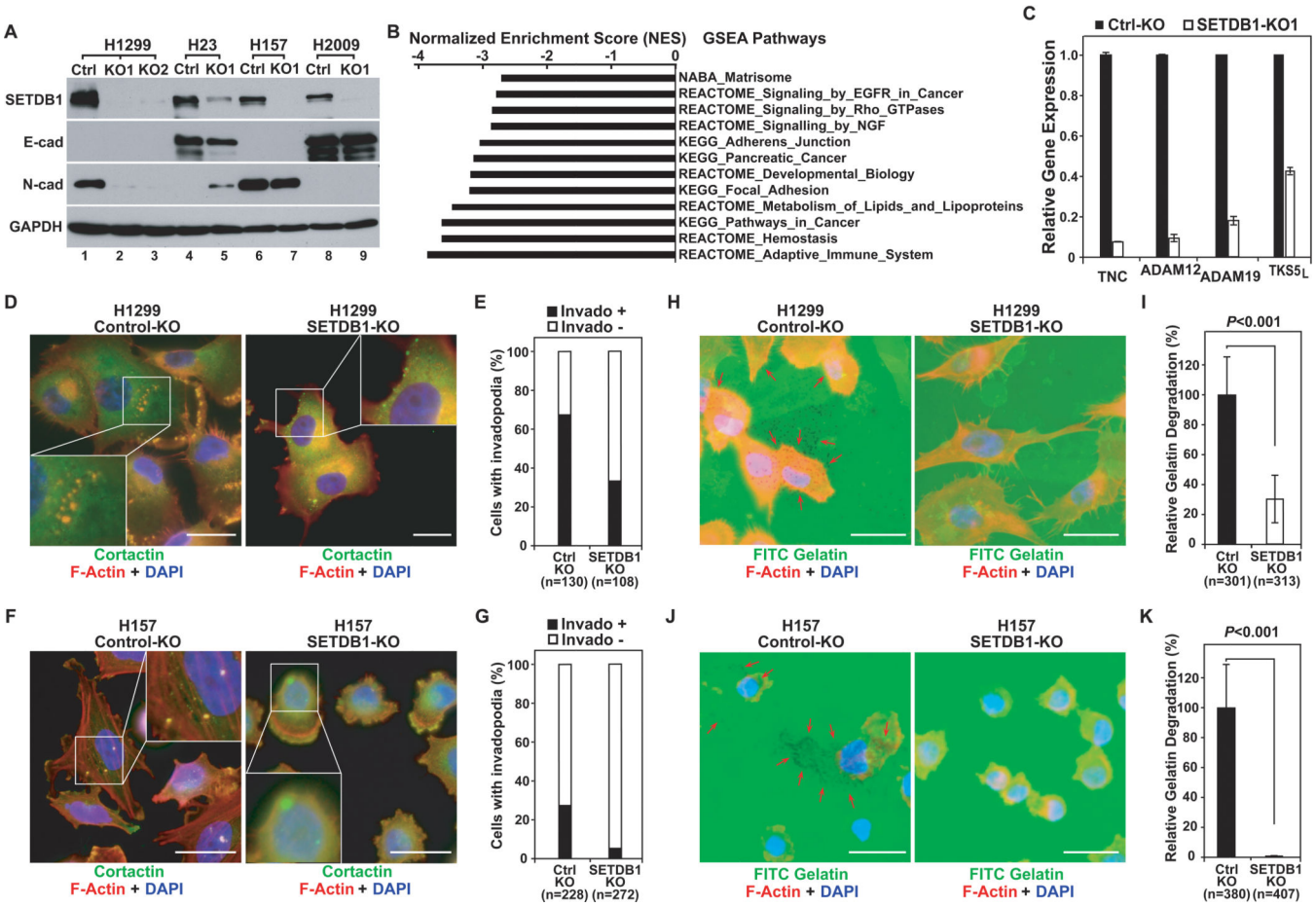

Figure 2.

SETDB1 promotes invadopodia formation and ECM degradation. **(A)** Western blot analysis of different control and SETDB1-KO NSCLC cells. **(B)** GSEA pathway analyses of differentially expressed genes derived from RNA-Seq data of control and SETDB1-KO H1299 cells. Top downregulated GSEA pathways with the best normalized enrichment score (NES) are listed. **(C)** RT–PCR analysis of indicated invadopodia-related genes in control and SETDB1-KO H1299 cells. Results are from triplicates and normalized to GAPDH (mean±s.d.). mRNA level in control cells were normalized as 1. **(D)** Representative merged immunofluorescent images of Cortactin (green), F-Actin (red) and DAPI (blue) co-stained control and SETDB1-KO H1299 cells. Enlarged images show Cortactin puncta with or without F-Actin. Scale bars indicate 20μm. **(E)** Quantification of control and SETDB1-KO H1299 cells with or without formed invadopodia structures. n is the number of cells counted. **(F)** Merged immunofluorescent images of control and SETDB1-KO H157 cells co-stained with Cortactin (green), F-Actin (red) and DAPI (blue), showing cells with or without invadopodia (inserted images). Scale bars indicate 20μm. **(G)** Quantification of invadopodia-containing control and SETDB1-KO H157 cells. n is the number of cells counted. **(H)** Representative merged images of FITC-Gelatin (green), F-Actin (red) and DAPI (blue) stained control and SETDB1-KO H1299 cells. Areas with FITC-gelatin degradation are indicated with arrows. **(I)** Quantification of areas with FITC-gelatin degradation in control

and SETDB1-KO H1299 cells. Results represent mean of 10 randomly picked areas with ±s.d. Control cells-mediated ECM degradation was normalized as 100%. n is the number of cells in all quantified areas. **(J)** Merged immunofluorescent images of control and SETDB1-KO H157 cells in FITC-gelatin degradation assays. Degraded areas are marked with arrows. **(K)** Quantification of ECM degradation mediated by control and SETDB1-KO H157 cells. n is the total number of cells counted.

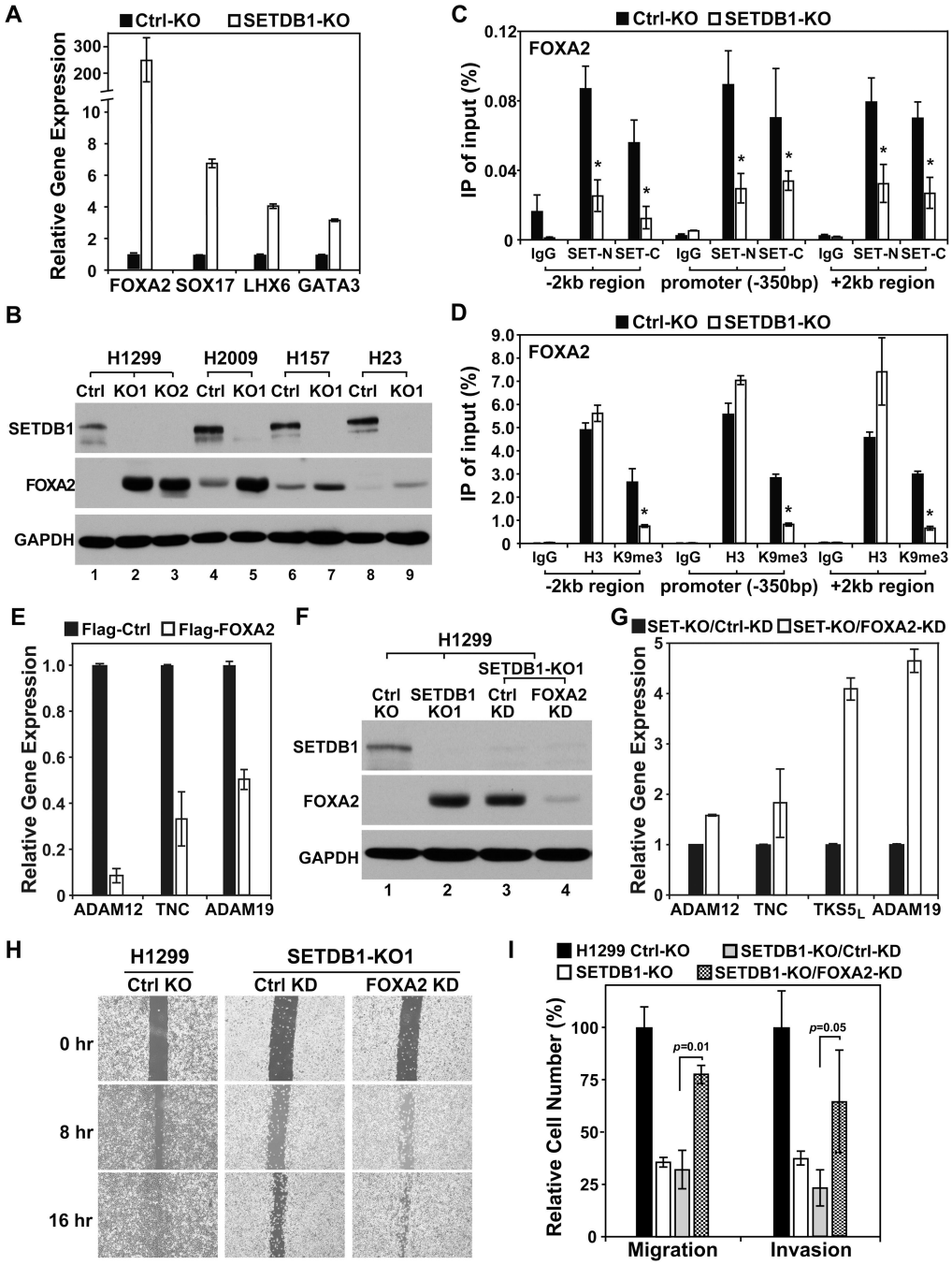

Figure 3.

SETDB1 represses FOXA2 to promote migration and invasion of NSCLC cells. **(A)** RT–PCR analysis of indicated genes in control and SETDB1-KO H1299 cells. Results were from triplicates and normalized to GAPDH (mean±s.d.). **(B)** Western blot analysis of SETDB1 and FOXA2 expression in indicated control and SETDB1-KO NSCLC cells. **(C)** ChIP-qPCR analysis of chromatin derived from control and SETDB1-KO H1299 cells. Antibodies against SETDB1 N- or C- terminal (SET-N, SET-C) were used for ChIP while qPCR was conducted using primers for FOXA2 promoter and −/+ 2kb regions. Graphs

are mean ChIP enrichment (n=3) with ±s.d. **(D)** ChIP-PCR analysis of same set of cells using antibodies for histone H3 and H3K9me3 and same primers for FOXA2 genomic locus. Graphs are mean ChIP enrichment (n=3) with ±s.d. **(E)** RT–PCR analysis H1299 cells expressing control or Flag-SETDB1. Results are from triplicates and normalized to GAPDH (mean±s.d.). **(F)** Western blot analysis of control and SETDB1-KO H1299 cells and SETDB1-KO cells with additional control or FOXA2 stable knockdown. **(G)** RT–PCR analysis of SETDB1-KO H1299 cells with control or FOXA2-KD. Results are from triplicates and normalized to GAPDH (mean±s.d.). **(H)** Wound-healing assays of control and SETDB1-KO H1299 cells with control or FOXA2-KD. Cell monolayers were treated with Mitomycin C (10 μg/ml) for 2 h before scratch. **(I)** Migration and invasion assays of control and SETDB1-KO H1299 cells and cells with additional control or FOXA2-KD. Cells were treated with 10 μg/ml Mitomycin C for 2 h before being seeded into transwell. Results are from three independent samples (mean±s.d.). Control-KO cells were normalized as 100% while *p* values were indicated.

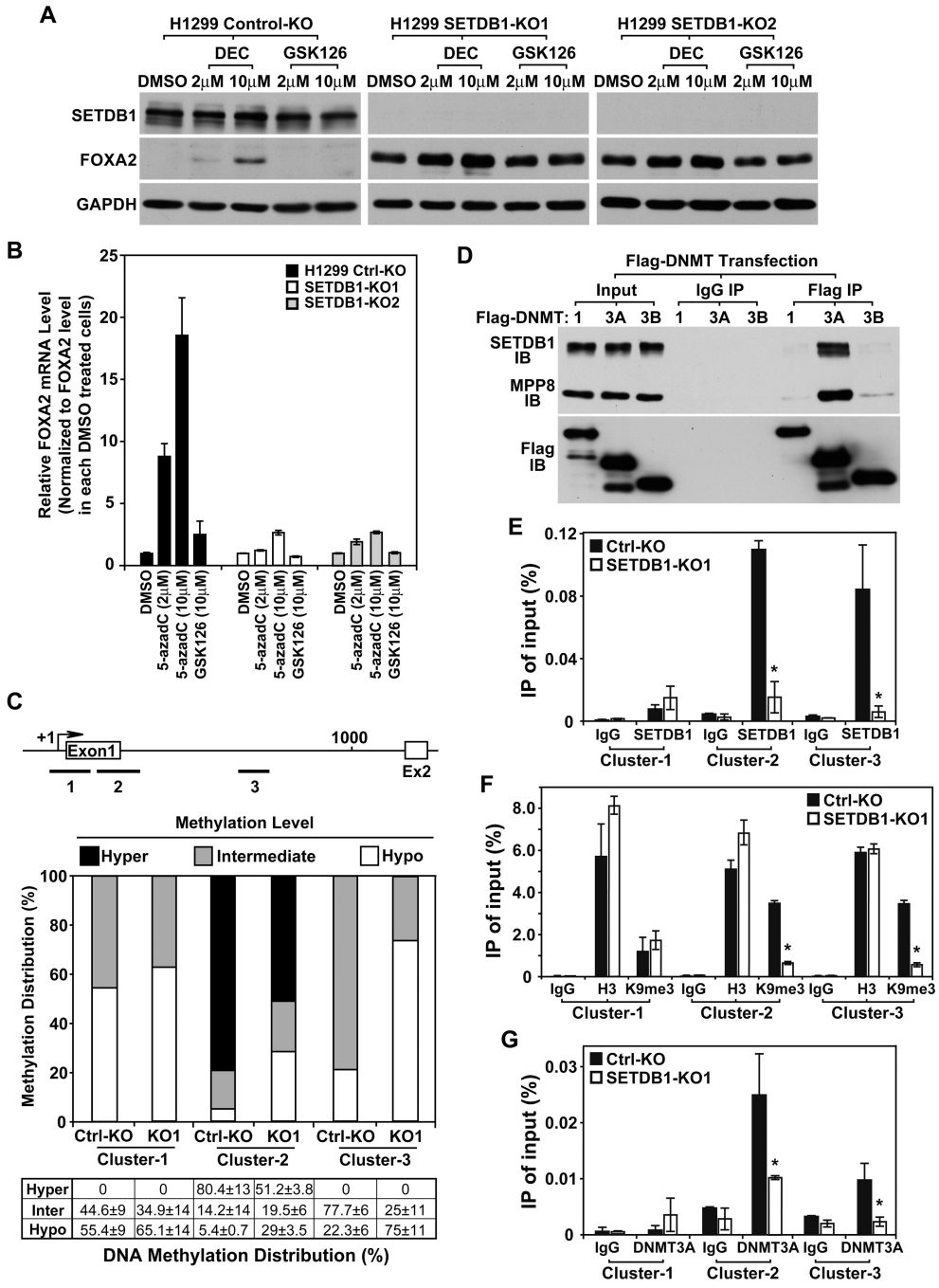

Figure 4.

SETDB1 cooperates with DNMT3A and DNA methylation for FOXA2 silencing. **(A)** Western blot analysis of control and SETDB1-KO H1299 cells treated with DMSO, decitabine (DEC) or GSK126 (72 h). **(B)** RT–PCR analysis of FOXA2 mRNA in control and SETDB1-KO H1299 cells with the same treatments. Results are from triplicates and normalized to GAPDH (mean±s.d.). FOXA2 level in DMSO-treated cells was normalized as 1. **(C)** MethylScreen assay of three indicated FOXA2 CpG clusters using genomic DNA derived from control and SETDB1-KO H1299 cells. White, black, and grey

boxes represent the unmethylated, uniformly methylated and partially methylated DNA proportions, respectively. Quantifications are from 3 independent samples (mean±s.d.) **(D)** HEK-293T cells were transfected with Flag-DNMT1, 3A, or 3B vectors followed by Flag-IP and western blot analysis of co-purified endogenous SETDB1 and MPP8 (top). IP efficiency was indicated by Flag western blot (bottom). **(E-G)** ChIP–PCR analysis of chromatin derived from control and SETDB1-KO H1299 cells. Antibodies against SETDB1 **(E)**, histone H3, H3K9me3 **(F)** or DNMT3A **(G)** were used for ChIP and qPCR was conducted using primers for different FOXA2 CpG clusters indicated in **(C)**. Results are mean ChIP enrichment (n=3) with ±s.d. * indicates $p<0.05$.

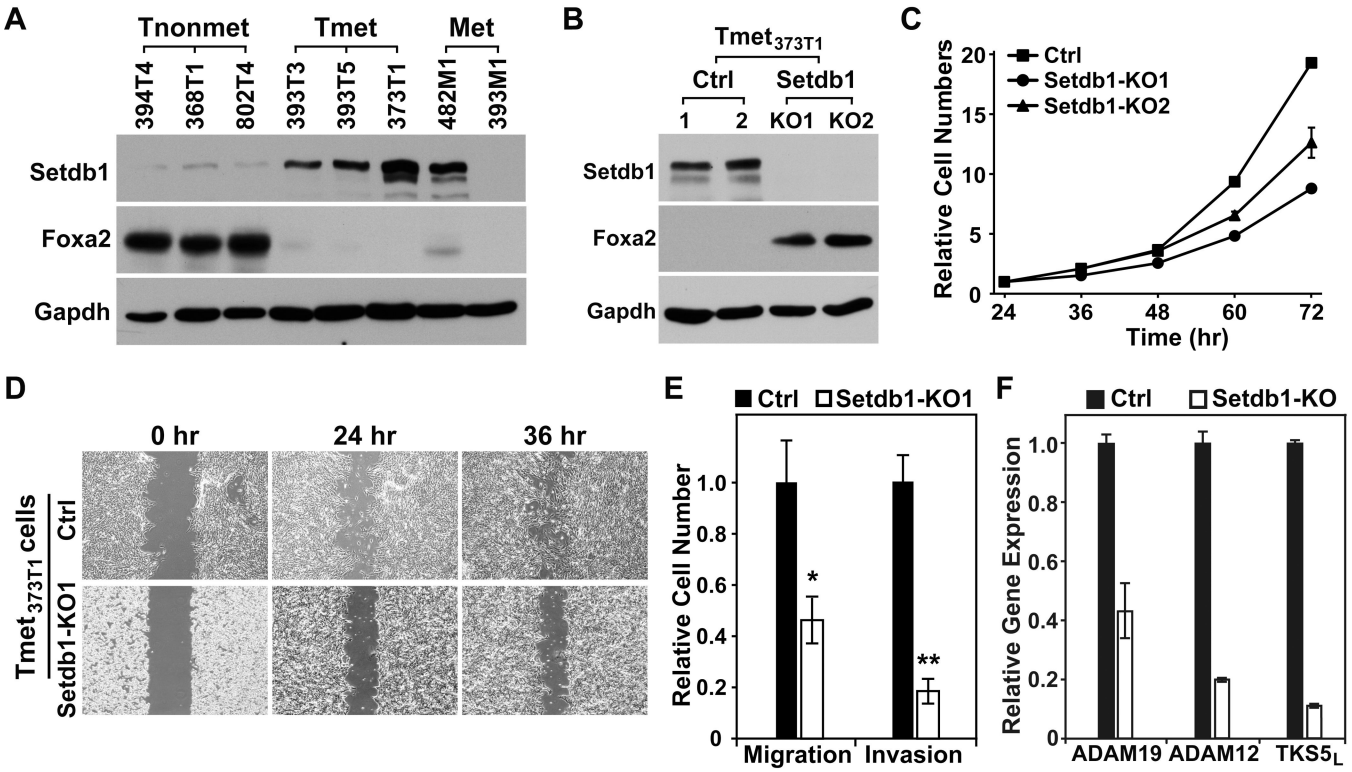

Figure 5.

Setdb1 represses Foxa2 expression and promotes motility and invasiveness of murine *Kras*$^{G12D/+}$;*p53*$^{fl/fl}$ lung adenocarcinoma cells. **(A)** Western blot analysis of a serial of cell lines derived from murine *Kras*$^{G12D/+}$;*p53*$^{fl/fl}$ lung adenocarcinoma model [26]. **(B)** Western blot analysis of indicated control and Setdb1-KO Tmet$_{373T1}$ cells. **(C)** Proliferation assay of control and Setdb1-KO Tmet$_{373T1}$ cells using Cell Counting Kit-8. Cell number 24 h after seeding was normalized as 1. Results were from three independent samples (mean±s.d.). **(D)** Wound-healing assays of control and Setdb1-KO Tmet$_{373T1}$ cells. Cell monolayers were treated with 10 μg/ml Mitomycin C for 2 h before scratch. **(E)** Migration and invasion assays of control and Setdb1-KO Tmet$_{373T1}$ cells. Cells were treated with Mitomycin C (10 μg/ml) for 2 h before being seeded into transwell. Graphs were from three independent samples (mean±s.d.). Control cells were normalized as 100%. * indicates p<0.01, ** indicates p<0.001. **(F)** RT-PCR analysis of control and Setdb1-KO Tmet$_{373T1}$ cells. Results were from triplicates and normalized to 18S rRNA.

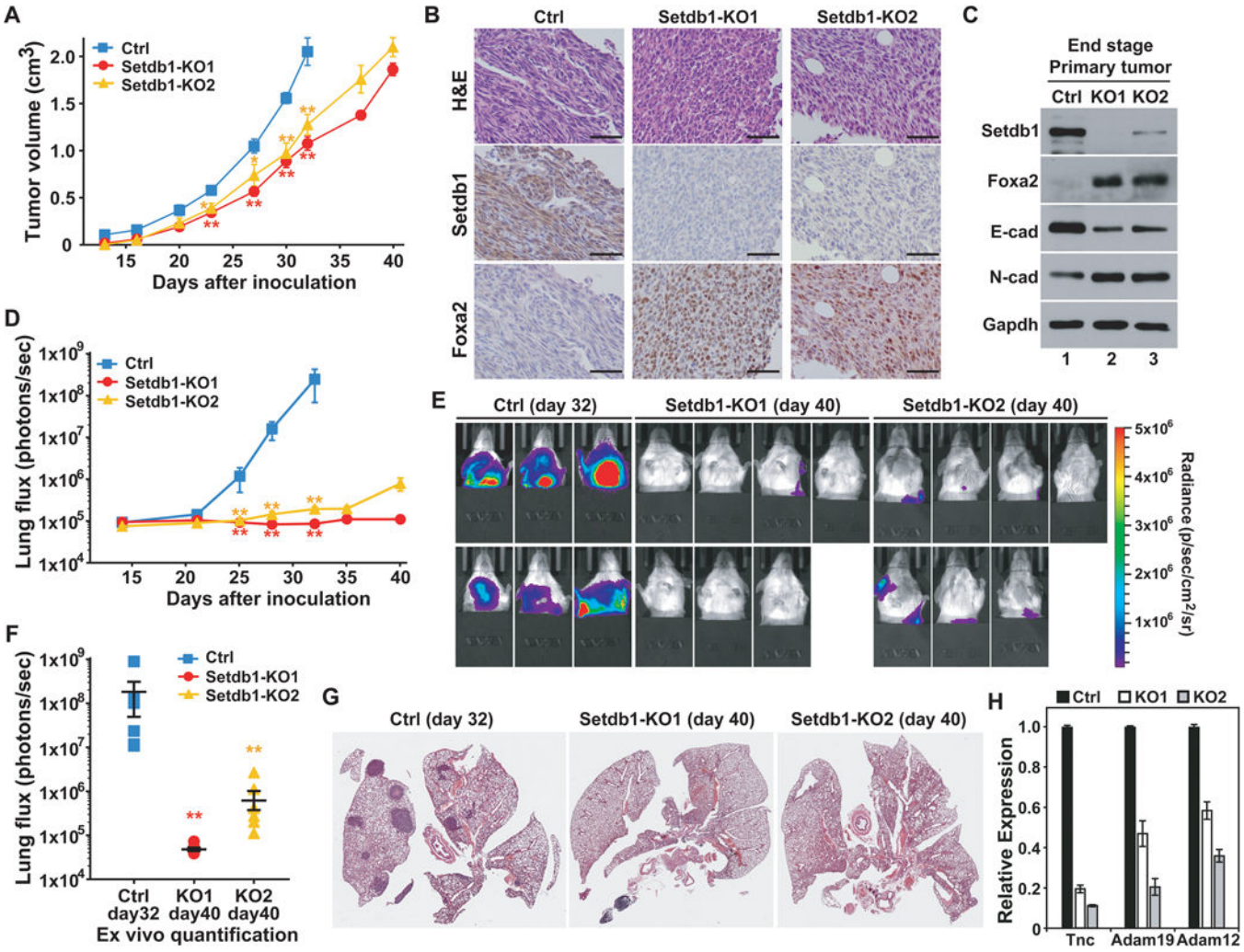

Figure 6.

SETDB1 promotes NSCLC malignant progression and metastasis. **(A)** Primary tumor growth (mean±SEM) measured by a caliper in SCID mice subcutaneously xenografted with control (n=6) or two different Setdb1-KO (n=7) $Tmet_{373T1}$ cells (~1.25×10^4) in a 32- or 40-day time course. * indicates $p<0.05$, ** indicates $p<0.005$. **(B)** Representative images of endstage control or Setdb1-KO $Tmet_{373T1}$ primary tumor sections stained with haematoxylin and eosin (H&E, top) or antibody against Setdb1 (middle) or Foxa2 (bottom). Scale bars are 50μm. **(C)** Western blot analysis of endstage primary tumors from control and Setdb1-KO $Tmet_{373T1}$ xenograft models. (**D**) Bioluminescence quantification of lung metastases (mean ±SEM) in subcutaneous xenograft models inoculated with control (n=6) and Setdb1-KO (n=7) $Tmet_{373T1}$ cells in a 32- or 40-day time course. ** indicates $p<0.005$. **(E)** Bioluminescence images of control and Setdb1-KO $Tmet_{373T1}$ xenograft mice at the endpoint. Primary tumors were covered to expose lung metastases. **(F)** Ex vivo bioluminescence quantification of dissected lungs (mean ±SEM.) from endstage mice xenografted with control (n=6) or Setdb1-KO (n=7) $Tmet_{373T1}$ cells. ** indicates $p<0.005$. **(G)** Representative images of H&E-stained whole lung sections derived from endstage control and Setdb1-KO $Tmet_{373T1}$ xenograft models. **(H)** RT-PCR analysis of control and

Setdb1-KO endstage control or Setdb1-KO $Tmet_{373T1}$ primary tumors. Results were from triplicates and normalized to 18S rRNA (mean±s.d.).